Appendix A. Deliverable 2.1, Milestone 2.1

Report of X-WiWa Database

Larsén X. G., Bolaños R., Jenkins A. D. and Tarp-Johansen N.J.
Prepared by Xiaoli Guo Larsén, 2014-08-08

The X-WiWa project so far has collected measurements or links to measurements in offshore conditions. The availability of the data has been made possible through public databases as well as connections to other (mostly European) projects. For the latter case, the use of the data should be acknowledged under the corresponding projects.

1. The big database

Figure 1 is a map of sites where data are available in the North Sea and Baltic Sea through the EU project InnWind. Figure 2 shows the sites where lidar measurements of wind are available through NORSEWIND project.
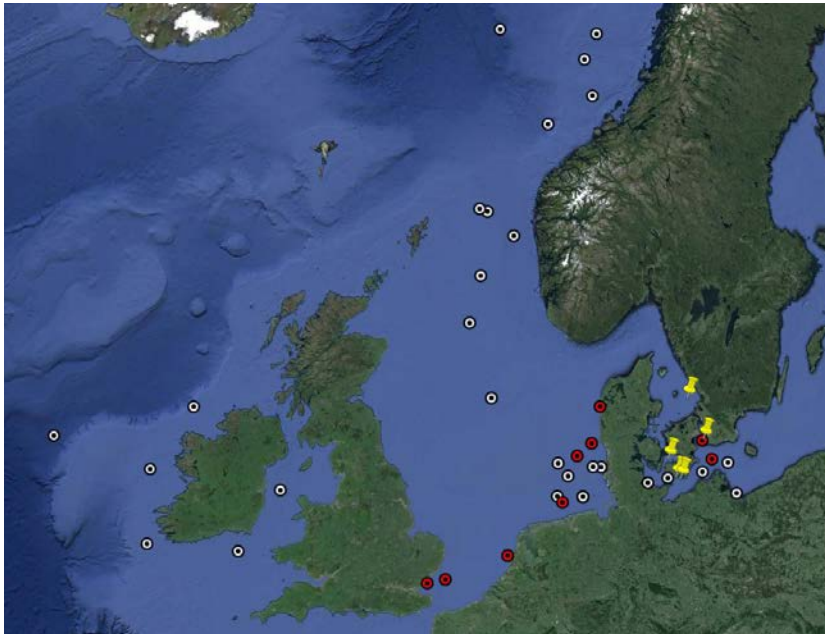
Fig. 1 A copy from Bastigkeit and Gottschall 2014 (Innwind project report D1.11: Database of existing wind parameter measurements for tall atmospheres across Europe): A map of all measurements locations in the North and Baltic Seas, available in InnWind databases. Their report also introduced: "the locations of buoy measurements (black/white points) and met masts (red and yellow markers) in the North and Baltic Sea are shown. The yellow markers signalise met masts where the access to the data depends on industrial owners".
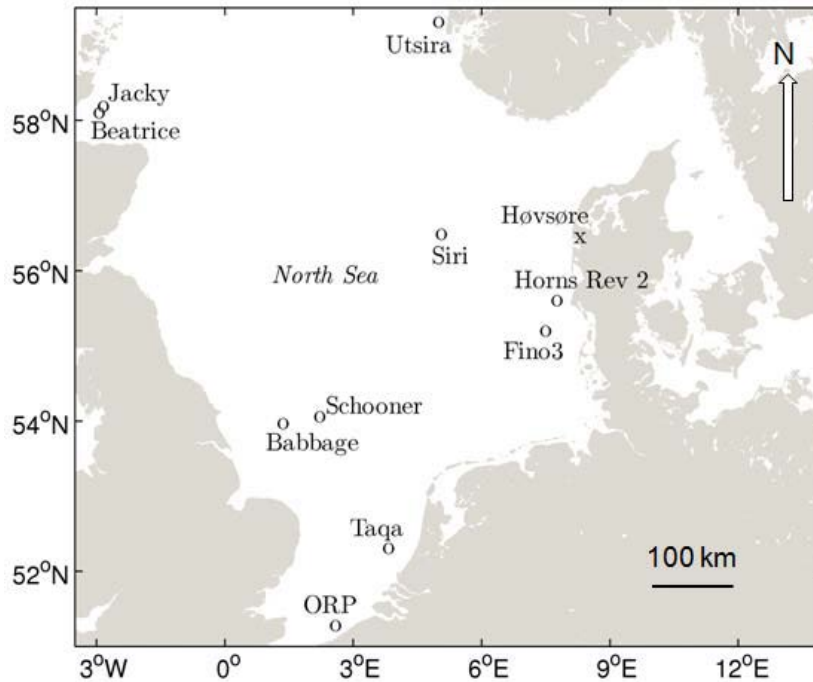
Fig. 2. A copy from Hasager et al. 2013 (Hub height ocean winds over the North Sea observed by the NORSEWInD LiDAR array: measuring techniques, quality control and data management. *Remote Sens.*, 5(9), 4280-4303; http://www.mdpi.com/2072-4292/5/9/4280)

2. Special databases

2.1. For case studies – Horns Rev and FINO 1 & 3

To make initial case studies, the case selection and data validation will be preliminarily based on the measurements from Horns Rev and the FINO sites. The availability of measurements at Horns Rev and FINO 1 & 3 can be found in Table 1.

Site	Lat	Long	Data Period	Data type
Horns Rev mast 2	*55.508*	*7.875*	*1999 – 2006*	*Standard, turbulence, wave*
FINO 1	*54.014*	*6.588*	*2004 – 2010*	*Standard Wave*
FINO 3	*55.195*	*7.158*	*2009 - now*	*Standard Wave*

Table 1. Basic information about the measurements from Horns Rev and FINO 1 and 3. "Standard" means standard meteorological measurements, "turbulence" means high frequency sonic measurements, "wave" means wave measurements.

Horns Rev is coastal, shallow water, site and the corresponding wind and wave conditions are challenging to model. It is the only offshore site in the Danish coastal waters we have turbulence wind measurements. In Table 2, a number of cases were selected for modeling tests based on measurements at Horns Rev. The rows marked with shadows are priorized due to the availability of turbulence and wave data. We have also collected a number of high resolution SAR maps (by Merete) for a limited number of dates as well as QuickSCAT data (by Ioanna) for the dates given in the table. The daily water temperatures at the Horns Rev site were also downloaded from satellite data for the period 1999 – 2006 (by Ioanna).

	Met	Tur	wave
20020127-29	Y	Y	Y
20020222-28	Y	N	Y
20021027-29	Y	N	Y
20031205-06	Y	Y	Y
20031214-16	Y	Y	Y
20031220-22	Y	Y	Y
20040319-22	Y	Y	Y
20041117-19	Y	N	Y
20061026-28	Y	N	N
20061207-12	Y	N	N

Table 2. Cases selected based on measurement availability from Horns Rev mast 2

More recent cases could of course be selected – but there won't be offshore turbulence data. The case 20061101, classified as the cold air case, identified at FINO 1, recommended by DONG, is also chosen.

2.2. RASEX database

The data are available for the two periods 19940516 to 19949528, and 199409 to 199410. They are available on Risø's database. There are probably no extreme weather cases there due to the season this period covers.

3. How the data have been used so far

The measurements from Horns Rev and FINO 1 have been used to help selecting the test cases. So far all experiments have been done to one case 20031214 – 16 (Table 2). This choice was taken before we got data from the FINO sites. A new test case 20040319 – 22 will be used because of the availability of data at FINO 1.

The data from Horns Rev (profile, tur, wave, water and satellite) have been used to validate the model outputs and they have been analyzed to understand the air-sea exchange processes.

The wave data from Horns Rev and FINO have been used to validate some wave modeling output to understand the extreme wave conditions.

4. Additional stations

Additional stations are listed in Table 3 to 5.

Table of wave data

Name	Instrument	Longitude	Latitude	Depth/elevation	Period	Variables
Dowsing	DWR	1,05316667	53,53133333	22 ?	Oct 2003 -Aug 2011	Hm0, Tp, Tz, Wdir
Ekofisk Laser		3,2114	56,5504	75 ?	1997 - 2009	Hm0, Tz
Ekofisk WR		3,2114	56,5504	75	1997 - 2009	Hm0, Tp, Tz, Wdir
Ekofisk					1980-1990	H4rms, Hmax
Ekofisk wave rider					1980 - 2000	
Fino 1		6,587667	54,014333	30?	2004 - 2010	Hm0, Tp, Wdir
Fino1	DWR	6,587667	54,014333	30	2003 - 2011	Hm0, Tp, Wdir….
Fino1 Wamos		6,587667	54,014333	30	2004 - 2010	Hm0, Tp, Wdir
Horns Rev 1					jan-07	Hm0, wind speed, wind dir
Horns Rev 2					Jan - Feb 2007	
K13 DWR		3,220278	53,217778	30	1978 - 2012	Hs, Tm0, Wdir
Nymindegab		7,9398	55,8090	46	1998 - 2008	Hm0, dir, Tz,Tp,
Fjaltring		8,0582	56,4750	-46,5	1992 - 2008	Hm0, dir, Tz, Tp
Laesoe Ost		11,5667	57,2167	70	oct 2005 dic 2005	Hm0, Tm0, Wdir
Laesoe South		11,1224117	57,0837330	0	1999 - 2000	Hmax, Hm0, Tz, Tp, Wdir
Tidsudtraek					2005 - 2006	Hm0, Tp, Tz,
West Silver Pit		0,625333	53,543333	19	2007 - 2009	Hm0, Tz, Tp,
Huvudskar East	Buoy	19,17	58,93	90	01-10-2004 - 07-12-2004	
Finngrundet	Waverider	18,61	60,90	70	10-10-2006 - 15-04-2008	
Arkona	Buoy	13,86	54,88	46	01-01-2007 - 15-04-2008	
Arkona	ADCP	13,8667	54,8833	46	01-01-2005 - 31-12-2005	
MS01	ADCP	11,3553	54,5859	21,2	07-03-2009 - On going	
MS02	ADCP	11,2880	54,5340	27	30-07-2009 - On going	
Nysted	ADCP	11,6627	54,5348	8,71	15-10-2004 - 31-10-2006	
MS01	Triaxys	11,3553	54,5859	21,2	10-06-2010 - 13-07-2010	
Sortegrund_WR		14,251767	55,238917	27	Feb - Dec 2005	Hs, Tp, Tz

Table 3. Stations of wave measurments.

Site	Latitude	Longitude	Period	Wind Instrument
Beatrice	58.108028	-3.069278	2010-11-10 – 2011-02-25	Wind lidar
Egmond	52.6064	4.38964	2005-07-01 – 2008-12-31	cup
FINO I	54.0002	6.59	2003-07-30 – 2010-05-01	cup
FINO II	55.0069	13.1542	2007-07-31 – 2010-04-30	cup
FINO III	55.195	7.1193	2009-09-01 - now	
Greater Gabbard	51.8727	1.91537	2006-01-23 – 2010-07-12	cup
Horns Rev I, M2	55.5191	7.78752	1999- 2006	cup
Horns Rev I, M6, M7	55.4873	7.9753	2005 - 2009	Cup
Horns Rev II	55.5996	7.6227	2009-06-25 – 2011-07-01	cup
Jacky	58.183869	-2.979842	2010-11-10 – 2011-11-09	Wind lidar
Lillegrund 1	55.5	12.76	2003-08-28 to 2006	cup

Lillegrund 2	55.4998	12.7654	2006-05-08 and on	cup
Omø	55.05	11.13	2002-08-23 - 2005-06-27	cup
Rødsand I	54.535	11.664	2004 - 2008	cup
Rødsand II	54.5734	11.4615	2009-12-14 and on	cup
Schooner	54.059161	2.076322	2010-07-16 and on	Wind lidar
Siri	56.4827	4.91117	2010-06-20 – 2011-05-02	Wind lidar
Store middel-grund	56.561	12.105	2008-11-18 and on	cup
Taga	52.3056	3.68519	2010-02-25 – 2011-03-19	Wind lidar
Utsira	59.3066800	4.85639146750	2009-09-28 – 2011-07-01	Wind lidar

Table 4. Stations of wind measurements part of these already included in Section 1)

Site	Public	Quality
Horns Rev	Risø has previously received. Whether they may share depends on the agreement with Leo Jensen	Good
FINO1 data	DONG Energy is not allowed to share it - Risø should have the data on their own	BSH is not happy with the Extreme events
Shell Flats / West of Duddon Sands	Not	Would be a combined set of wind and wave measurements from two positions some kilometres apart. There has been some uncertainty about the wind. Calibration is taking place. Wave heights are good. Probably fair to combine the data sets.
Horn Sea	Not	Risø is familiar with the data
London Array	Not	To be investigated. Probably poor.

Table 5. A few sites DONG Energy has access to the data (by Niels Jacob Tarp-Johansen)

Appendix B. Milestone M1.4

M1.4
"Subroutines in MIKE SW to estimate the parameters to be transferred to the atmosphere model"

The approach tested during the first stage of the X-WiWa project was through the exchange of roughness length from MIKE SW to WRF. MIKE SW uses Janssen (1991) formulation which provides a roughness length estimate. Additional formulations were considered (Fan, 2012; Liu, 2011). These are described in the following:

Janssen (1991)

Within the Janssen (1991) theory, the Charnock parameter is dependent on the wave induced stress which at the same time it is dependent on the wind input source term in a spectral wave model formulation. The Charnock parameter is defined as:

$$\frac{g z_0}{u_*^2} = \frac{\alpha}{\sqrt{1 - \dfrac{\tau_w}{\tau}}} \quad \text{where } \alpha = 0.01$$

And the wave stress is estimated from the wind input source function as

$$\tau_w = \int d\omega d\theta \frac{K}{\omega} S_{in}$$

Where S_{in} is the wind input source function in energy balance equation as described in Janssen (1991, 2004).

Fan et al. (2012)

They simulated 29 years of waves using a coupled HIRAM-WWIII model. In the coupled system the roughness length is feedback to the atmospheric model as lower boundary condition. They reported that the WWIII formulation gave values of z_0 of more than 0.012 m while a new formulation was of 0.003 m. The new z_0 formulation depends on wind speed and wave age ($c_p/u*$) described as

$$Charnok = \frac{z_0 g}{(u_*)^2} = a \left(\frac{c_p}{u_*} \right)^b$$

Where a and b are fitting constant at nine different wind speed ranging from 10 to 50 m/s:

$$a = \frac{0.023}{(1.0568)^{u_{10}}}$$

$$b = 0.012 u_{10}$$

The above equations are solved together with:

$$u_z = \frac{u_*}{k} \ln \left(\frac{z}{z_0} \right)$$

Liu et al. (2011)

They use a Charnock relation that takes into account the wave state and the sea spray effects based in (Liu et al., 2008). Atmosphere-Wave coupling showed to strengthen the tropical cyclone while the thermodynamic coupling weakens it. The formulation is defined as follow:

$$Charnok\ coef = \frac{z_0 g}{u_*^2} = \begin{cases} (0.085(\frac{c_p}{u_*})^{\frac{3}{2}})^{1-(\frac{1}{\omega})}\left[0.03(\frac{c_p}{u_*})e^{-0.14c_p/u_*}\right]^{1/\omega}, & \sim 0.35 < \frac{c_p}{u_*} < 35 \\ \\ 17.6^{1-(\frac{1}{\omega})}(0.008)^{1/\omega}, & \frac{c_p}{u_*} \geq 35 \end{cases}$$

c_p is the phase speed at the peak of the spectrum, $\omega = \min(1, a_{cr}/ku*)$ is the correction parameter indicating the influence of sea spray on the logarithmic wind profile, k= von Karman constant, a_{cr}=0.64 m/s is the critical value of terminal fall velocity of droplets.

The roughness due to molecular viscosity Zs is also added to the sea surface roughness:

$$z_s = \frac{0.11\vartheta}{u_*}, \quad \vartheta = kinematic\ molecular\ viscosity\ of\ air$$

The WRF – MIKE 21 SW coupling was tested in a first phase in an offline mode. This means that only MIKE 21 SW was transferred towards WRF. Janssen estimates of roughness were provided by the model while estimates using Fan and Liu formulations were done outside the model (via Matlab). Matlab functions were created for this purpose (see appendix).

A comparison of both formulations for a series of different wind speed (U_{10}) and wave celerity (c_p) (Figure 1) showed that Liu (2011) formulation provided a wider range of values, some probably to high compared to some observation and thus Fan (2012) was chosen as a first option for evaluation. However, further investigation on Liu (2011) formulation should be done as it could explain part of the large scatter typically observed in measurements.
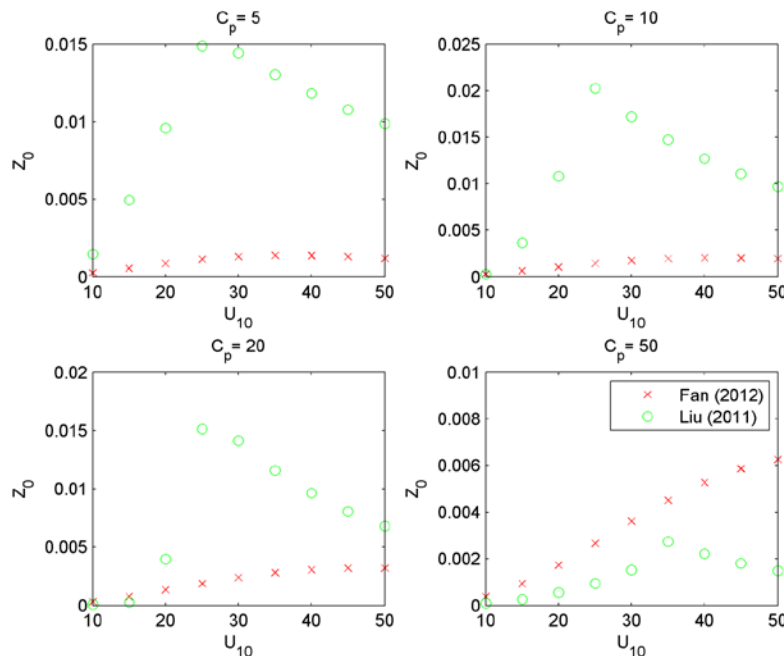

Figure 1. Z_0 estimates using Fan (2012) and Liu (2011) for different combinations of wind speed (u_{10}) and wave celerity (c_p).

References

Janssen, P.A.E.M., 1991. Quasi-linear theory of wind generation applied to wave forecasting. Journal of Physical Oceanography 21, 1631-1642.

Fan, Y., Lin, S.J., Held, I.M., Yu, Z., Tolman, H.L., 2012. Global ocean surface wave simulation using a coupled atmosphere-wave model. Journal of Climate 25, 6233-6252.

Liu, B., Guan, C., Xie, L., 2008. Investigating the impacts of wave state and sea spray on typhoon via coupled atmosphere-wave system: the idealized case. , 28th Conf on hurricane and tropical Meteorology. Amer. Meteor. Soc, Orlando, Fl.

Liu, B., Liu, H., Xie, L., Guan, C., Zhao, D., 2011. A coupled atmosphere-wave-ocean modeling system: Simulation of the intensity of an idealized tropical cyclone. Monthly Weather Review 139, 132-152.

Appendix

```matlab
function z0=RoughFan(Cp,U10)
% to estimate sea surface roughness according to Fan et al (2012)
% dependent on wave age

a=0.023./(1.0568.^U10);
b=0.012.*U10;
k=0.4;  % von karman constant

%Cp=10;   %  m/s
Ust=.01;  %just a value to start interation

   % Fan et al (2012)
for i=1:8; % interations
    Z0=a.*((Cp./Ust).^b).*(Ust.^2)./9.81;
    Ust=U10.*k./log(10./Z0);
end
z0=Z0;
_____
function z0=RoughLiu(Cp,U10,option)
% to estimate sea surface roughness according to Liu et al (2011)
% dependent on wave age
%option=1 if u10 is provided, =2 if u* is provided

acr=0.64; % m/s fall velocity of droplets
k=0.4;  % von karman constant

if option==1  % when providing u10
%Cp=10;   %  m/s
%Ust=.01;  %just a value to start interation
Cd=(0.8 + (0.065.*U10)) .* (10.^-3); % from Wu (1980)
Ust=sqrt(Cd).*U10; % To start interations with a more realistic Ust

[x y]=size(U10);
for m=1:x
    for n=1:y

     for i=1:8; % interations
         w(m,n)=min([1 acr./(k.*Ust(m,n))]);
           if Cp(m,n)./Ust(m,n)<35 & Cp(m,n)./Ust(m,n)>0.35
               Z0(m,n)=([[0.085.*((Cp(m,n)./Ust(m,n)).^(3/2)))^(1-
(1./w(m,n)))].*[0.03.*(Cp(m,n)./Ust(m,n)).*exp(-
0.14.*Cp(m,n)./Ust(m,n))].^(1/w(m,n))).*(Ust(m,n)^2)./9.81;
           else    %elseif Cp(m,n)./Ust(m,n)>=35
               Z0(m,n)=((17.6.^(1-
(1./w(m,n)))).*(0.008^(1./w(m,n)))).*(Ust(m,n).^2)./9.81;
           end
         Ust(m,n)=U10(m,n).*k./log(10./Z0(m,n));
     end
    end
```

```matlab
        end
end

elseif option==2 %  when providing u*
    Ust=U10;
    [x y]=size(U10);
for m=1:x
    for n=1:y
    %  for i=1:8; % interations
        w(m,n)=min([1 acr./(k.*Ust(m,n))]);
            if Cp(m,n)./Ust(m,n)<35 & Cp(m,n)./Ust(m,n)>0.35
                Z0(m,n)=([[(0.085.*((Cp(m,n)./Ust(m,n)).^(3/2)))^(1-
(1./w(m,n)))].*[0.03.*(Cp(m,n)./Ust(m,n)).*exp(-
0.14.*Cp(m,n)./Ust(m,n))].^(1/w(m,n))).*(Ust(m,n)^2)./9.81;
            else    %elseif Cp(m,n)./Ust(m,n)>=35
                Z0(m,n)=((17.6.^(1-
(1./w(m,n)))).*(0.008^(1./w(m,n)))).*(Ust(m,n).^2)./9.81;
            end
    %      Ust(m,n)=U10(m,n).*k./log(10./Z0(m,n));
    % end

    end
end
end
z0=Z0;
_____

function L=WaveLength(T, h)
% calculate wave length from period and depth
%
%T=4;
%h=5;

Ltemp = 9.81.*(T.^2)./(2.*pi);

for j=1:5
    Ltemp=[9.81.*(T.^2)./(2.*pi)] .* tanh(2.*pi.*h./Ltemp);

end
L=Ltemp;
```

Appendix C. An overview of the model couplers for X-WiWa

Jianting Du

2014-08-05

A coupler is a software package that links media interactions between different model components in the Earth System Model(ESM). Typically, a coupler carries out functions of data exchange, grid interpolation and remapping. This document provides a short overview of the main coupling technologies including ESMF, MCT, MCEL, OASIS and OpenMI.

1 ESMF

The Earth System Modeling Framework (ESMF) is an established multi-agency collaboration (NASA/NSF/DOE/NOAA) component framework started from 2002. The core development team was located in NCAR and then moved to NOAA/CIRES. It began in the global weather and climate modeling community, now includes coastal, hydrological, and space weather applications. Until February 2014, ESMF has 76 Model Components which are included in 13 Coupled Modeling Systems. It has full Fortran 90 interface and partial C/C++ interface. It runs on most high performance parallel computing platforms, including IBM, many Linux variants, Cray, Compaq, etc. It supports MPI, OpenMP and hybrid user codes. The current release is Version 7.0 beta(July 3, 2014).

ESMF is comprised of a superstructure for coupling Earth system components that wraps user code with minimal overhead, and an infrastructure for building Earth system components, including time manager, data structures for storage and manipulation, parallel data communications and regridding software, message logging tools and resource file manager. Components can operate concurrently or sequentially, in one or limited multiple executables. Its component wrappers may be layered on top of other coupling technologies (e.g. MCT, FMS). ESMF provides many tools or functions such as a broad range of time management functions, Python interface for grid remapping, standalone application that can generate interpolation weights in parallel, various regridding methods, incorporation with NCL for regridding, Web service interface. It also includes attribute packages that can be used to store, aggregate and output model metadata which allowing the model to essentially document itself.

Timing results for a variety of codes show that the sparse matrix multiply approach and basic component wrappers scale to tens of thousands of processors. Grid remapping and parallel communications are also fast and scalable. A comparison in CCSM4 indicates that ESMF is as efficient as MCT.

In order to adopt ESMF, modelers arrange their code as a set of Gridded Components and Coupler Components, and then split these components into standard ESMF methods (initialize, run, and finalize). The next steps are to wrap native model data structures with ESMF data structures, and then register components with the framework. These wrapped components can then be called by a driver, which can be user-customized, to form a coupled application. Since ESMF is a very large package, the users will take significant effort in order to master the software.

2 MCT

The Model Coupling Toolkit(MCT) is a set of open-source software tools for creating coupled models developed by Argonne National Laboratory. The first version of MCT worked on paralleling CCSM coupler(cpl5-cpl6) in 2000. Its later version(MCT2.0 – MCT2.7.3) played a central role in the CCSM3 and CCSM4/CESM1. MCT has also been used to form other coupled systems such as COAWST, WRF/ROMS Hurricane model, COAMPS-ROMS. ESMF is very well documented, supported and maintained. The latest version is MCT2.8.3(Dec 17, 2012).

MCT is not a coupling framework, but a set of open-source software tools for creating coupled models. MCT provides a Fortran-based object model for coupling construction; the bindings for C++ and Python have been developed. Supported platforms include IBM (Power and BG/P), Cray XT*, Linux clusters (with Absoft, GNU, Lahey, NAG, PGI, PathScale, or Intel compilers and MPICH, OpenMPI, VMI and/or ChaMPIon/Pro MPI libraries), NEC.

MCT provides the following core coupling services: A component model registry, domain decomposition descriptors, communications schedulers for parallel M x N intercomponent data transfer and M x M intracomponent data redistribution, a flexible and indexible (i.e., random-access) field data storage datatype, a time averaging and accumulation buffer datatype, a general spatial grid representation capable of supporting unstructured grids, parallel tools for intergrid interpolation implemented as matrix-vector multiplication spatial integration and averaging tools (including paired integrals to support conservative interpolation), tools for merging data from multiple components for use by another component, a programming model similar to that of the Message Passing Interface, MCT can be used in single or multiple executable systems and allows sequential or concurrent execution.

MCT offers a fully parallel implementation of coupling field regridding and transformations via Message Passing Interface (MPI). Its sparse matrix multiply approach is used by many other couplers such as ESMF, OASIS, CPL7, etc.

The biggest challenge in using MCT is defining linearization of mesh and index spaces. Most new MCT users, however, quickly build their own parallel coupled models after experimenting with the examples provided. Ease of use is the primary benefit of MCT. Its limitations are lack of support for computation of interpolation weights and for MPI communicator construction.

3 MCEL

The Model Coupling Environmental Library (MCEL) was developed to simplify the coupling process for models that exchange data at most every time step, with funding from the U.S. Department of Defense High Performance Computing Modernization Program in 2003. MCEL coupling has been implemented in various coupling models such as WRF-SWAN(Gorman and Neilson,1999, Booij et al., 1999, Ris et al., 1999), WRF-WAM(Jenkins, 2011, Jenkins et al., 2012). MCEL is a Fortran based coupler, supports multi languages such as C++, Java, Python, etc. The architecture of data transformation between model components is client-filter-server. The centralized server stores cou-

pling information, while clients (numerical models) store and retrieve data from server. Data passes through filter between server and client for interpolation, data combination, physics, etc. The drawback of MCEL is its less efficiency due to the client-server architecture. And it is also lack of funding and support for maintenance and improvement.

4 OASIS

The OASIS coupler is developed by CERFACS since 1991. One of the most widely used version is OASIS3 due to its great flexibility and its low intrusiveness in the component codes. OASIS3 is used today by about 35 different climate modelling groups in Europe, Australia, Asia and North America. Parallelism and efficiency drove the developers designed OASIS4. However, they stopped developing newer version and started to collaborate with MCT to develop a new version – OASIS3-MCT which made OASIS3 a fully parallel coupler. The usage of OASIS3-MCT in the component code has largely remained unchanged with respect to OASIS3.3. To communicate with another model, or to perform I/O actions, a component model needs to include a few specific calls to the OASIS3-MCT coupling library, using the same API as in OASIS3.3. The scalability tests done with OASIS3-MCT at high number of cores and the fact that it supports unstructured grids proved that it is now a fully parallel and efficient coupler.

5 OpenMI

The Open Modeling Interface (OpenMI) has been developed in order to link together model components from various origins. OpenMI provides a standard model interface, a reference implementation of that standard, and utilities to support existing models in adhering to that standard. The first version of the Open Modeling Interface (OpenMI) was launched at the end of 2005. Science 2007, a core group of six institutes has worked on an upgrade of the OpenMI towards version 2.0. The complaint components of OpenMI are mostly hydrological models such as DHI models. One of the advantage in OpenMI is that it allows models running on different platforms(e.g. Windows, Unix and Linux). A successful example is the coupling between Weather Research and Forecast (WRF) atmospheric model and Soil and Water Assessment Tool (SWAT 2012) hydrological model using OpenMI 2.0 and ESMF web-service module which enables climate model runs on a high performance computer while the hydrologic model runs on a personal computer.

6 Discussion

The document provides an overview of the current model couplers. Each coupler has its advantages and disadvantages. ESMF contains the most breadth of functions. It is efficient, portable, flexible, well supported and widely adopted. Since it is a large package that encompasses many functions and features, users can expect a significant learning curve to master the software. Moreover, coupling systems using ESMF are too complex (e.g. GEOS-5, CESM1) to be used as reference. Considering that the aim of X-WiWa project is coupling atmospheric and wave models for storm conditions. It is not necessary to use such a large package as the coupler. However, some of the ESMF tools could be used as auxiliary functions. On the contra-

ry, MCT is a small package which is easy to use, its efficiency, portability, flexibility are similar to or better than ESMF. What's more, there are some good examples (e.g. COAWST, WRF-ROMS) for us to learn its usage. It meets with the requirements of X-WiWa. The apparent defect of MCEL is its rather low efficiency, which makes it not suitable for high resolution simulation. There is no obvious defect in OASIS3-MCT. But since I am not an experienced user of OASIS, it does not have obvious attraction to me. OpenMI is a good coupler or Interface in coupling hydrological models. A benefit is that some staffs in DHI are OpenMI committee members. We could get some help from them if we use OpenMI. But the efficiency and usage of OpenMI still need further evaluation.

Reference

[1]   Valcke, S., Balaji, V., Craig, a., DeLuca, C., Dunlap, R., Ford, R. W., … Vertenstein, M. (2012). Coupling technologies for Earth System Modelling. Geoscientific Model Development, 5(6), 1589–1596. doi:10.5194/gmd-5-1589-2012

[2]   Dunlap, R., Rugaber, S., & Mark, L. (2010). A Feature Model of Coupling Technologies for Earth System Models Feature Analysis of Coupling Technologies, 1–25.

[3]   Cerfacs, S. V., Dunlap, R., & Tech, G. (2011). Coupling Technologies for Earth System Modelling : Today and Tomorrow, 8–66.

[4]   Dunlap, R., Vertenstein, M., Valcke, S., & Craig, T. (2014). Second Workshop on Coupling Technologies for Earth System Models. Bulletin of the American Meteorological Society, 95(2), ES34–ES38. doi:10.1175/BAMS-D-13-00122.1

[5]   Web Page(ESMF): http://www.earthsystemmodeling.org/

[6]   Collins, N. (2005). Design and Implementation of Components in the Earth System Modeling Framework. International Journal of High Performance Computing Applications, 19(3), 341–350. doi:10.1177/1094342005056120

[7]   Joint, E., Team, S., Boville, B., Cheung, S., Clune, T., Craig, T., … Young, M. (2014). Earth System Modeling Framework ESMF Reference Manual for Fortran.

[8]   Craig, A. P., Vertenstein, M., & Jacob, R. (2012). International Journal of High Performance Computing Applications modeling developed for CCSM4 and CESM1. doi:10.1177/1094342011428141

[9]   Craig, T. (n.d.). CPL7 User' s Guide.

[10]   Liu, F. (2012). Performance measurement of remapping code in CESM coupler using MCT and ESMF sparse matrix multiply (SMM): Part 1 performance analysis on 1024 processors 1 . Experiment Setup, 2–6.

[11]   Liu, F. (n.d.). Performance measurement of remapping code in CESM coupler using MCT and ESMF sparse matrix multiply (SMM): Part 2 scaling performance analysis 1 . Experiment Setup, 2–5.

[12]   Web page(MCT): http://www.mcs.anl.gov/research/projects/mct/

[13]   Larson, J. (2005). The Model Coupling Toolkit: A New Fortran90 Toolkit for Building Multiphysics Parallel Coupled Models. In-

ternational Journal of High Performance Computing Applications, 19(3), 277–292. doi:10.1177/1094342005056115

[14]   Jacob, R. (2005). M x N Communication and Parallel Interpolation in Community Climate System Model Version 3 Using the Model Coupling Toolkit. International Journal of High Performance Computing Applications, 19(3), 293–307. doi:10.1177/1094342005056116

[15]   Jacob, R. L., Ong, E., & Loy, R. (n.d.). The Model Coupling Toolkit API Refer- ence Manual : MCT v . 2 . 8.

[16]   Warner, J. C., Sherwood, C. R., Signell, R. P., Harris, C. K., & Arango, H. G. (2008). Development of a three-dimensional, regional, coupled wave, current, and sediment-transport model. Computers & Geosciences, 34(10), 1284–1306. doi:10.1016/j.cageo.2008.02.012

[17]   Warner, J. C., Armstrong, B., He, R., & Zambon, J. B. (2010). Development of a Coupled Ocean–Atmosphere–Wave–Sediment Transport (COAWST) Modeling System. Ocean Modelling, 35(3), 230–244. doi:10.1016/j.ocemod.2010.07.010

[18]   Jenkins, A. D., Paskyabi, M. B., Fer, I., Gupta, A., & Adakudlu, M. (2012). Modelling the Effect of Ocean Waves on the Atmospheric and Ocean Boundary Layers. Energy Procedia, 24(January), 166–175. doi:10.1016/j.egypro.2012.06.098

[19]   Jenkins, A. D. (2014). WRF-WAM coupling with MCEL

[20]   Web page(OASIS):https://verc.enes.org/oasis

[21]   Development, M. (2010). Model Development OASIS4 – a coupling software for next generation earth system modelling, 87–104.

[22]   Valcke, S. Craig, T. Coquart, L. (2013). OASIS3-MCT User Guide.

[23]   Web page(OpenMI): http://www.openmi.org/

[24]   Goodall, J. L., Saint, K. D., Ercan, M. B., Briley, L. J., Murphy, S., You, H., … Rood, R. B. (2013). Coupling climate and hydrological models: Interoperability through Web Services. Environmental Modelling & Software, 46, 250–259. doi:10.1016/j.envsoft.2013.03.019

Appendix D: **Nested offline coupling experiments**

Jianting Du, Xiaoli Guo Larsén, Rodolfo Bolaños Sanchez

This report is a summary of nested offline coupling experiments using WRF and MIKE 21 SW. The main purpose of this study is to investigate the impacts of nesting and different roughness length z_0 formulations on the wind field in the offline coupling model. The second purpose is to investigate the remapping approach between nested regular meshed WRF and unstructured meshed MIKE 21 SW. Section 1 describes the methodology and settings of the nested offline coupling. Section 2 demonstrates the application of the model and present results for an application to simulate a storm case.

1. Methodology

The schematic diagram of the offline coupling is described as Fig. 1. First of all, we run WRF to generate 10 meters wind velocity U_{10}. Then we converted it into a "dfsu" file using a Matlab program. The "dfsu" file were used as input to MIKE 21 SW to generate integral wave items such as peak frequency (Tp) and model parameters such as roughness length z_0 (Jenssen,1991)[1]. For the other formulations such as Fan et al. 2012[2], z_0 were calculated outside MIKE from wave age in terms of Tp, U_{10}, etc. More details about the z_0 formulations are given in the appendix. Then we converted z_0 into an intermediate file format which were used by "metgrid.exe" in WPS. This was done by a series of steps using NCL. Finally we run WRF with the new z_0 which is correlated with wave status at each iteration step of WRF.
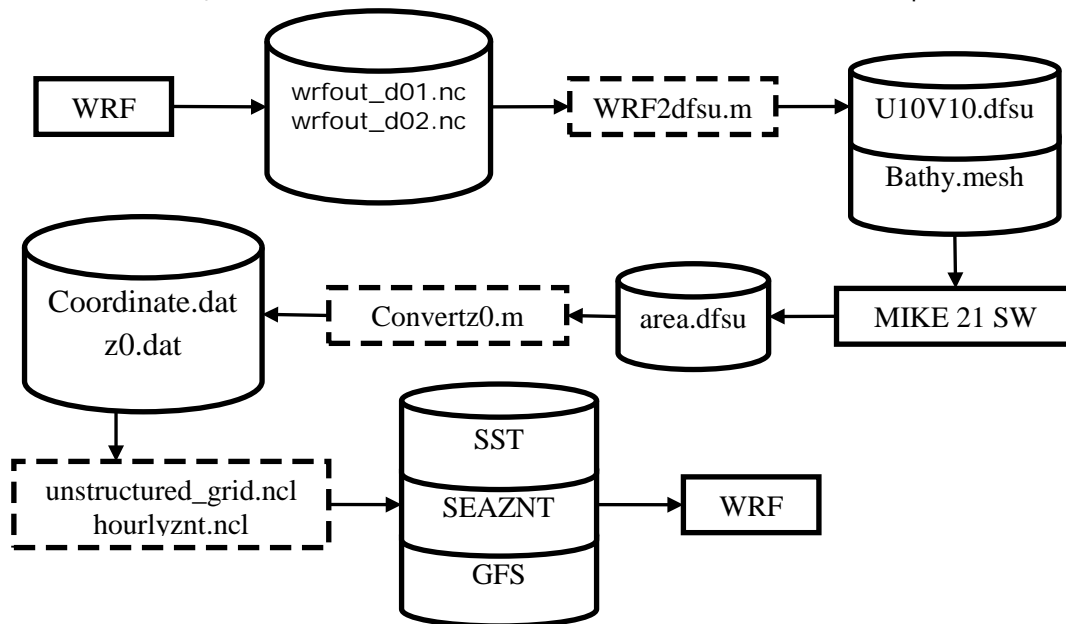

Fig. 1. A schematic diagram of the offline coupling using WRF and MIKE 21 SW. In the diagram, the arrows indicate the prognostic variables that are passed between the model components, the cylinders indicate data, the dished rectangles indicate programs for data conversion and the solid rectangles indicate model components.

WRF was set as two nested domains with regular mesh in lambert map projection, while MIKE was set as unstructured mesh in longitude-latitude map projection. In order to allow models to exchange data fields on different grids, a remapping approach was implemented here. Fig. 2 shows an example of the remapping. The MIKE grids points that are inside the WRF inner domain (domain 2) were interpolated from WRF grid points. The MIKE grid points that are in the WRF outer domain only were interpolated from grid points in WRF domain 1, and vice versa. As WRF domain 1 is larger than MIKE domain, when z_0 is interpolated into WRF grids, only the points inside MIKE domain were interpolated. Outside MIKE domain, the values will be supplemented by the default option 0(COARE3.0)[3] in WRF.
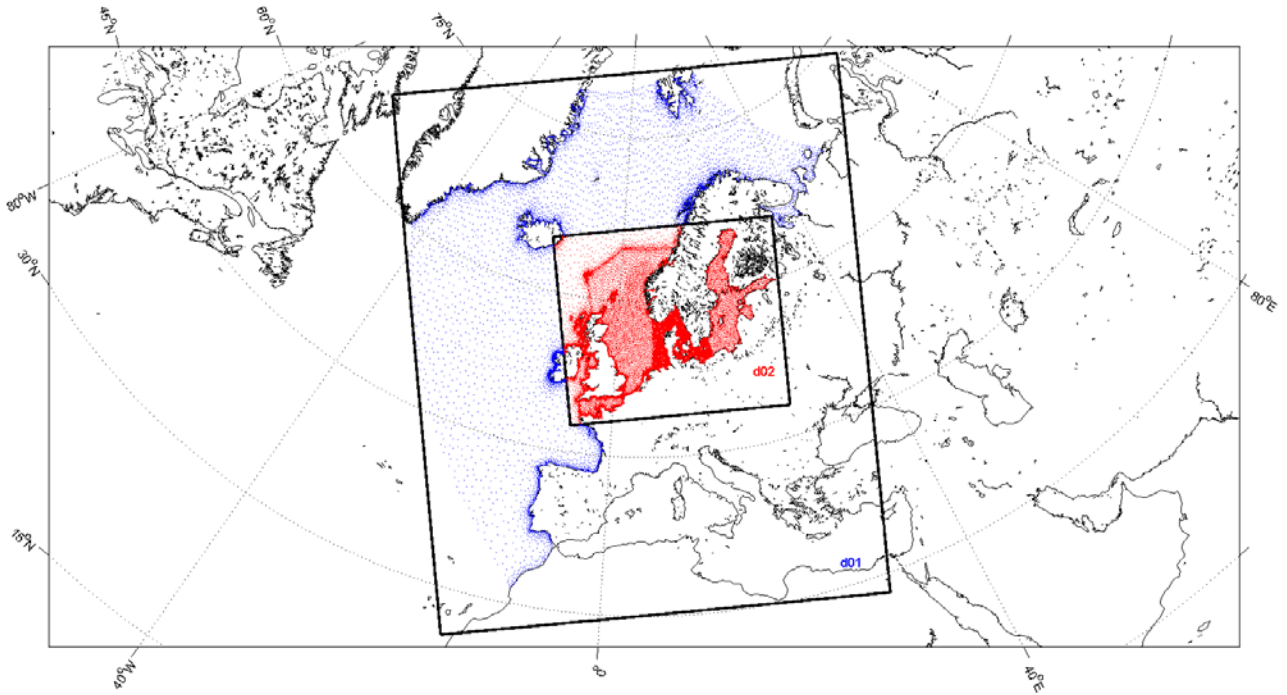
Fig. 2. Grid remapping between WRF and MIKE. The red points are the grid points of MIKE 21 SW that are inside the WRF inner domain, the blue points are in the WRF outer domain only. The black boxes are the domains in WRF.

2. Application and results

Initial and boundary conditions for the atmosphere model were obtained from global forecasting system (GFS) 1 degree data NCEP Final Analysis (http://dss.ucar.edu/datasets/ds083.2/). Additional boundary conditions for sea surface temperature were obtained from NCEP Real-Time Global, SST High-Resolution (RTG_SST_HR) analysis (ftp://polar.ncep.noaa.gov/pub/history/sst). The WRF model was two-way nested. The parent grid has 320X385 cells in the east-west and north-south direction with a resolution of 15 km. The child grid has 469X403 cells at a 5km resolution. As for comparison, a one-domain experiment was implemented with the same resolution as the child grid, 5 km.

The initial condition for the wave model was computed by JONSWAP spectrum. The unstructured grid was generated by MIKE Zero Mesh Generator.

Both WRF and MIKE were used to simulate from 00:00 December 14th 2003 to 00:00 December 15 2003. WRF used 41 vertical levels and has a time step of 60 seconds. The time step for MIKE varies from 600 seconds to 0.01 seconds.

With the above settings, 6 experiments were set up and run with different nesting and z_0 approaches. Table 1 summarizes the differences.

Table 1. Experimental designs.

Experiment	Domain	z_0 approach
Exp. 1	One domain	Option 0
Exp. 2	One domain	Fan et al.
Exp. 3	One domain	Jenssen
Exp. 4	Nested	Option 0
Exp. 5	Nested	Fan et al.
Exp. 6	Nested	Jenssen

2.1 Influence of nesting

As long as the coupling happens at the interface of the air and sea, it is particularly important to examine 10 meters wind speed U_{10} because it is used to drive the wave model and directly

influenced by the feedback of the roughness length z_0. The comparison of U_{10} between the one-domain and nested experiments are shown in Fig. 3. Here we choose 16:30 December 14th 2003 U_{10} as an example. The wind speed was North-west then turn to West. Nested experiments show more atmospheric oscillation details than one domain experiments. That means the nesting enables the model capture more atmospheric oscillation.

Fig. 3(a) and Fig. 3(b), Fig. 3(c) and Fig. 3(d) are U_{10} with the z_0 formulation of Option 0 and Fan et al. The comparison of the four subplots shows that more momentum was transferred from the boundary to the inner domain by means of nesting. Fig. 3(e) and Fig. 3(f) are using Jenssen's z_0 formulation. On the contrary, the comparison shows that less momentum was transferred from the boundary in the nested case. Why the nesting makes momentum transfer increase in some cases while decrease in another case? This "self-contradiction" performance could be explained from the U_{10} distribution of the outer domains. Fig. 4 shows the comparison of the U_{10} in the outer domains between Fan et al. and Jenssen's z_0 formulation. In the Fan et al.'s case, the outer domain resulted in a higher wind speed. It means that it provided a high wind speed boundary for inner domain which is higher than the wind speed of GFS boundary in one-domain case. Thus the nested inner domain got more momentum from the boundary. On the contrary, in the Jenssen's case, the outer domain provided a low wind speed boundary which is lower than the wind speed of GFS boundary in one-domain case. Thus the nested inner domain got less momentum from the boundary. It seems that the nesting amplifies the influence of z_0 on U_{10}. If the roughness length formulation is good, the nesting makes the result better. If the z_0 formulation is bad, the nesting makes the result worse. The underlying reason for this phenomenon is that the nesting enables the model solves the physical equation more accurate.
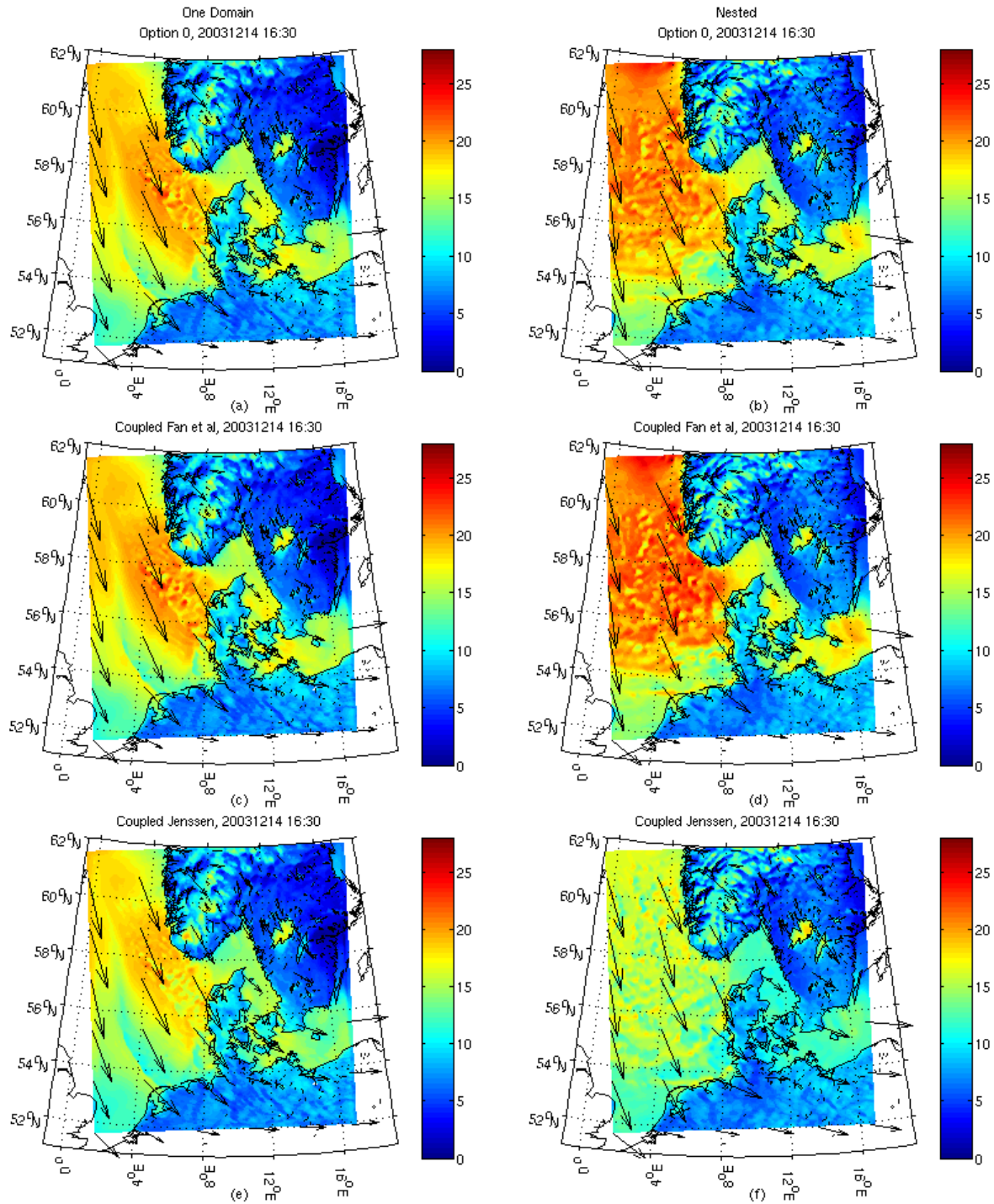
Fig. 3 Comparison of one-domain experiments and nested experiments. The three subplots on the left side (Including (a), (c) and (e)) are 10 meters wind speed U_{10} from one-domain experiments. The others on the right side (Including (b), (d) and (f)) are from nested experiments. Option 0, Fan et al. and Jenssen are corresponding to different roughness length formulations.
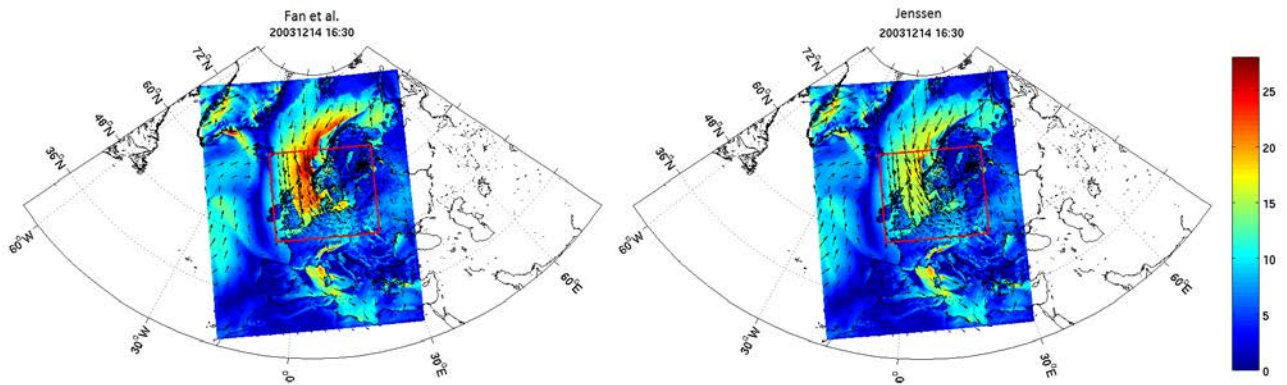
Fig. 4. Comparison of the 10 meters wind speed U_{10} in the outer domain between different roughness length formulations. The left subplot used Fan et al.'s formulation. The right one used Jenssen's formulation. The red rectangular in the middle is the boundary between the two domains.

2.2 Influence of different z_0 formulation

Fig. 5 shows the distribution of roughness length z_0 generated by different formulations in the experiments 4-6. Option 1[4,5] and Option 3[6] were not included in the experiments, but calculated after the simulation. The details about the z_0 formulations are given in the appendix. Jenssen's z_0 formulation was used in MIKE 21 SW to parameterize the wind input source function. The z_0 over ocean grows rapidly with wind speed at high wind speed. Though the others are of the same order of magnitude, their distribution varies from one to another. Fig. 5(f) shows z_0 as a function of 10 meters wind speed U_{10}, Fan et al.'s z_0 formulation which is coupled with wave model is less dependents on U_{10}, but the tendency are similar to the others.

Fig. 6 shows the influence of z_0 on U_{10} in experiments 4-6. U_{10} is basically inversely proportional to z_0. Fig. 6(b) and Fig. 6(d) shows the difference in U_{10} between Option 0 and Fan et al.'s z_0 formulation, and the difference between Option 0 and Jenssen's z_0 formulation. Fan et al. and Option 0's results are similar. But Jenssen's formulation resulted in a lower wind speed. Fig. 7 shows the comparison of U_{10} between model results and QuickScat measurements at 05:20 14th 2003 and 19:10 14th 2003. Obviously both Fan et al. and Option 0's results are close to the measurements but Jenssen's are quite different. Is that means Jenssen's formulation was wrong? Subplot Fig. 6(f) shows the scatterplot of U_{10} from coupled experiments vs U_{10} from uncoupled experiment. Though in subplot Fig. 5(f), Jenssen's z_0 shows very large difference from the others, in subplot Fig. 6(f) it shows much smaller difference. At low wind speed condition, the bias is ignorable. The difference is mainly at the wind speed lager than 15m/s. So Jenssen's z_0 formulation performs well at low wind speed but less well at high wind speed. And this experiment is about offline coupling which is physically not complete. The performance of Jenssen's z_0 formulation needs to be reassessed in the future. Anyhow, the advantage of Jenssen's formulation is that it based on the assumption that the total stress balances the wave-induced stress and the turbulent stress. It uses the same z_0 in both the atmospheric model and the wave model which is not considered in others. It promoted a good view of the coupling scheme which follows the energy conservation law.
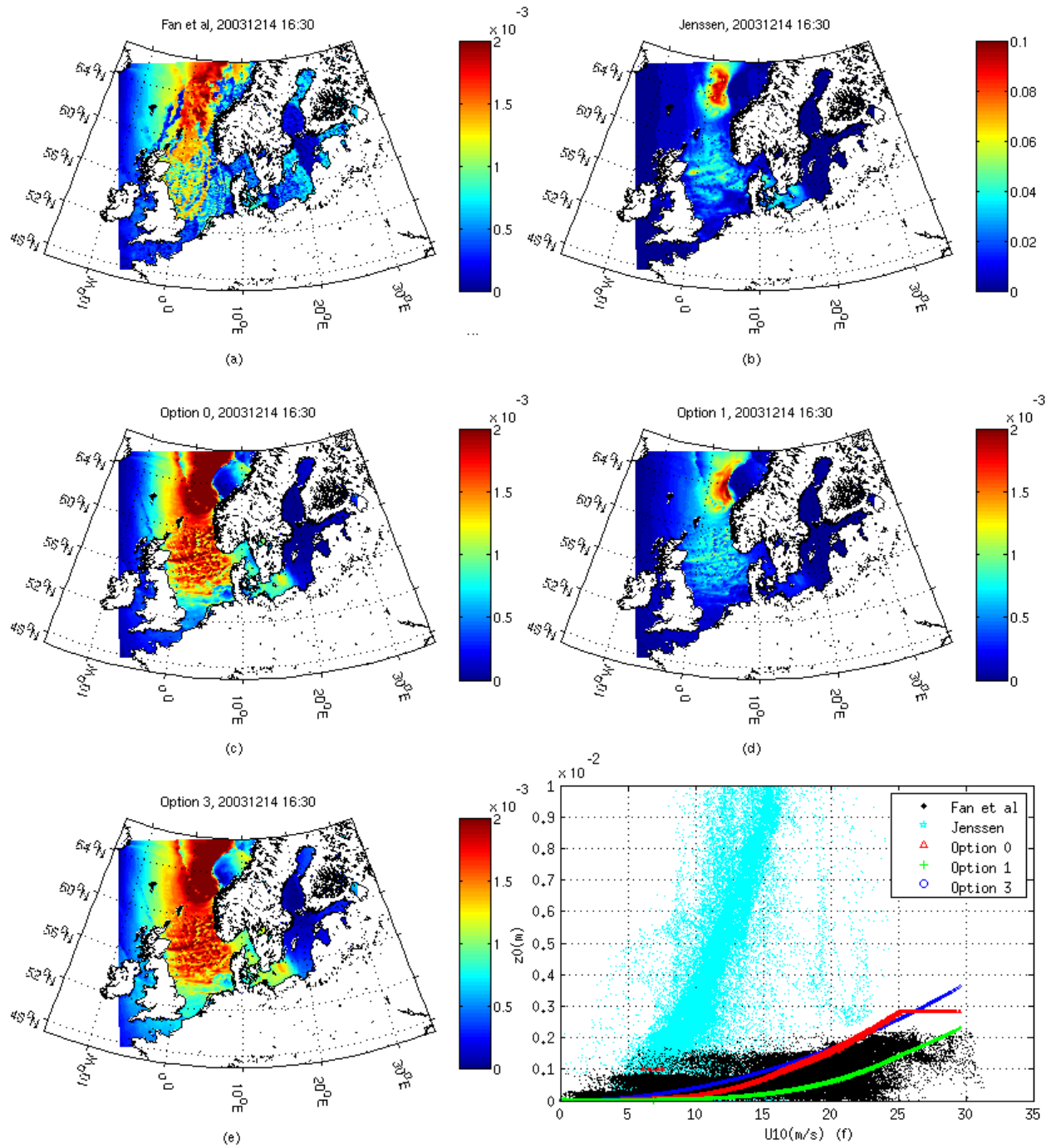
Fig. 5 Distribution of roughness length z_0 generated by different z_0 formulations at 16:30 December 14th 2003. Subplot (a)-(e) are the distribution of z_0. Subplot (f) is the scatterplot of z_0 as a function of 10 meters wind speed U_{10}.
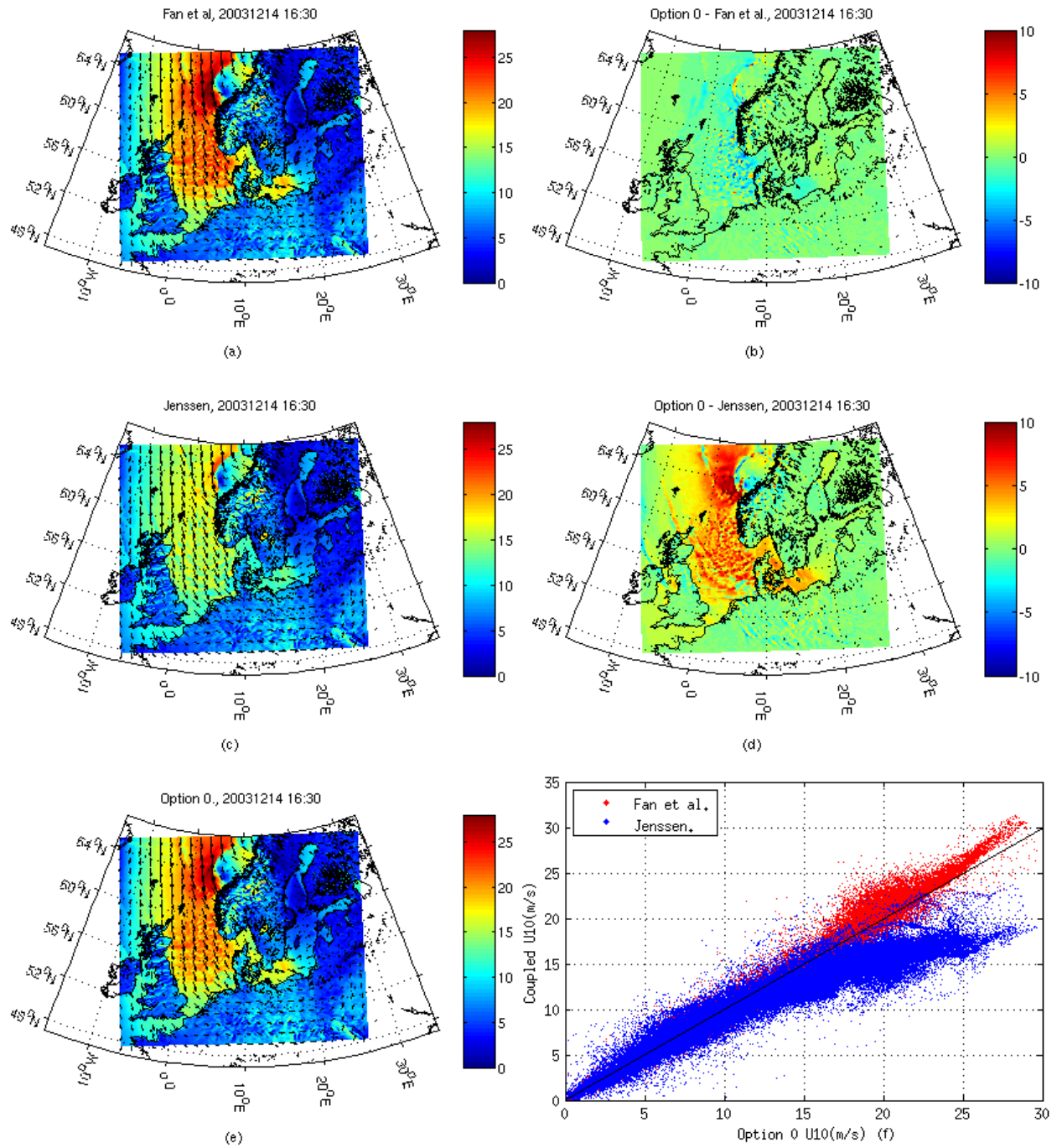
Fig. 6 Comparison of 10 meters wind speed U_{10} using different z_0 formulations at 16:30 December 14th 2003. Subplot (a), (c) and (e) are the distribution of U_0 using different z_0 formulations. Subplot (b) and (d) are the U_{10} of Option 0 minus U_{10} of Fan et al. and Jenssen. Subplot (f) is the scatterplot of U_{10} from coupled experiments vs U_{10} from uncoupled experiment.
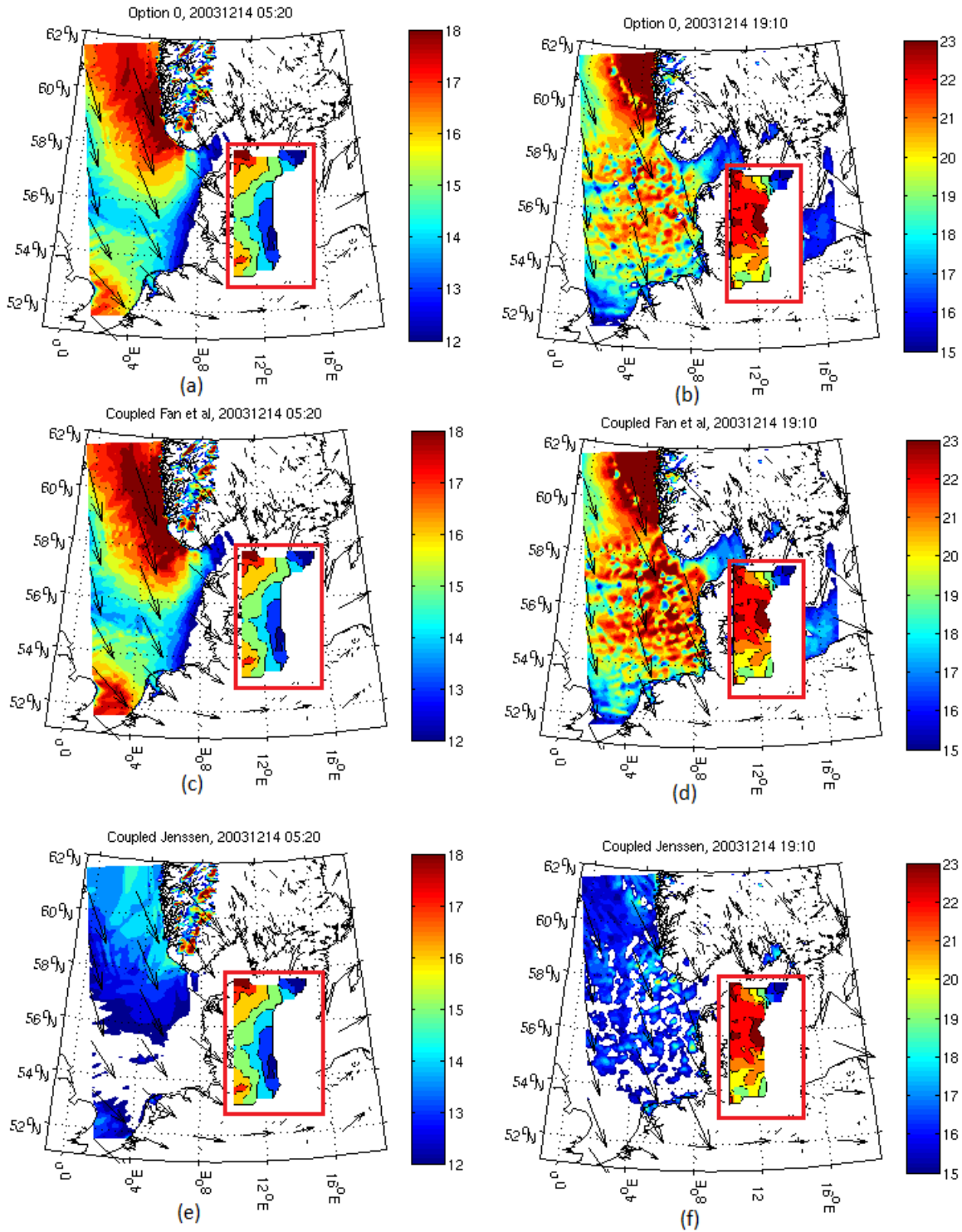
Fig. 7 Comparison of 10 meters wind speed U_{10} between model results and QuickScat measurements. The 3 subplots on the right side are at time 05:20 14th 2003, while on the left side are at time 19:10 14th 2003. The QuickScat U_{10} are placed at the red rectangles on the right side of the target place. The color-bars of the left subplots are different from the right ones because they have to match the color-bars of the QuickScat plots. So the wind speed under the minimum values of the color-bars is not shown (12m/s on the left and 15m/s on the right).

3. Discussion

This report summarizes the ongoing works on nested offline coupling. Though the operating is cumbersome it achieves the main purpose of the investigation of the impacts of nest and different roughness length formulations. Another achievement is we found the way of remapping between the two models.

Seemingly, the nesting enables the WRF model capture more atmospheric oscillation. Meanwhile it makes the influence of roughness length on 10 meters wind speed more obvious than using one domain. Both of the phenomenon reflect the fact that the nesting enables the model solve the physical equation more accurate. Jenssen's roughness length formulation shows a rougher sea surface than others, and it results in an obvious decrease of 10 meters wind speed in high wind speed condition. But it doesn't mean that Jenssen's roughness length formulation is wrong. One reason is that offline coupling is not good enough to capture the physics of coupling. More cases should be tested in online coupling. Another import aspect is that Jenssen's formulation enables the atmospheric model and the wave model uses the same z_0 which is not considered in the other formulations. And it promotes a good view of the coupling scheme which follows the energy conservation law.

1.1 Appendix: Roughness length formulation

The 5 different roughness length formulations are given briefly.

A1. Jenssen's fomulation

The default MIKE 21 SW roughness length is given by Jenssen (1996)'s formulation[1]. We only get through the main points of the approach.

Jenssen's formulation is based on the assumption that total stress т balances the wave-induced stress τ_w and the turbulent stress τ_{turb}:

$$\tau_w(z = z_0) + \tau_{turb}(z = z_0) = \tau$$

The roughness length z_0 is from Charnock relation (Charnock 1995):

$$z_0 = \alpha U_*^2 g,$$

where Charnock parameter α on the wave-induced stress:

$$\alpha = \beta \left(1 - \frac{\tau_w}{\tau}\right)^{-1/2}, \beta = 0.01,$$

where the surface stress $\tau = \rho_a U_*^2$, and ρ_a is the air density. The friction velocity $U_* = C_d^{1/2} U_{10}$, and the drag coefficient Cd is given as $C_d = (\kappa/\ln(L/z_0))^2$ With κ the von Kármán constant.

τ_w is named wave-induced stress which is a function of wind input source term S_{in} in wave model.

$$\tau_w = \rho_w g \int dw\, d\theta S_{in}/c$$

A2. Fan et al.'s formulation

Assuming the mean wind profile is close to logarithmic:

$$U_{10} = \frac{U_*}{\kappa} \ln\left(\frac{10}{z_0}\right)$$

From Moon et al. (2004), the Charnock parameter is fitted by the wave age:

$$\alpha = \frac{z_0 g}{U_*^2} = a\left(\frac{C_p}{U_*}\right)^b,$$

where the fitting coefficient $a = \frac{0.0023}{1.0568^{U_{10}}}, b = 0.0012 U_{10}$.

A3. Option 0

Option 0 is the default setting in WRF. z_0 are from COARE3.0(Coupled Ocean-Atmosphere Response Experiment)[3]:

$$z_0 = \frac{\alpha u_*^2}{g} + \frac{0.11\mu}{u_*},$$

where the Charnock parameter α increases linearly from 0.011 at $U_{10,n}=10 ms^{-1}$ to 0.018 at $U_{10,n}=18 ms^{-1}$ and remains constant for other cases.

A4. Option 1

In Option 1, z_0 is originated from [4] with some update based on the relation of the drag coefficient with wind speed from lab experiments of [5]. The formulation is:

$$z_0 = \left(1 - \left(\frac{u_*}{1.06}\right)^{0.3}\right)\left(\frac{0.011u_*^2}{g} + 1.59 \cdot 10^{-5}\right)$$
$$+ \left(\frac{u_*}{1.06}\right)^{0.3}\left(10exp\left(-9.5u_*^{-1/3}\right) + \frac{0.11 \cdot 1.5 \cdot 10^{-5}}{u_*}\right)$$

A maximum and minimum value of z_0 was set based on the lab data from [5]: $2.85 \cdot 10^{-3}$ and $0.125 \cdot 10^{-6}$ m.

A5. Option 3

In Option 3, z_0 is a function of wave steepness:

$$z_0 = 1200 \cdot h_s \left(h_s/L_p\right)^{4.5},$$

where h_s is the significant wave height and L_p is the wave length associated with the peak of the wave spectrum. H_s was formulated from [6]:

$$h_s = 0.0248 \cdot U_{10}^2$$

and

$$L_p = g T_p^2/(2\pi),$$

where T_p is the dominant wave period and it is calculated as

$$T_p = \begin{cases} 0.729 \cdot U_{10}, & U_{10} > 0.1 ms^{-1} \\ 0.1, & U_{10} \le 0.1 ms^{-1} \end{cases}$$

The upper and lower limits of z_0 are the same as Option 1.

1.2   Reference

[1] Janssen, Peter AEM, and Pedro Viterbo. "Ocean waves and the atmospheric climate." *Journal of climate* 9.6 (1996): 1269-1287.Fan, Yalin, et al. "Global ocean surface wave simulation using a coupled atmosphere-wave model." *Journal of Climate* 25.18 (2012): 6233-6252.

[2] Fan, Yalin, et al. "Global ocean surface wave simulation using a coupled atmosphere-wave model." *Journal of Climate* 25.18 (2012): 6233-6252.

[3] Fairall, C. W., et al. "Bulk parameterization of air-sea fluxes: Updates and verification for the COARE algorithm." *Journal of climate* 16.4 (2003): 571-591.

[4] Davis, Christopher, et al. "Prediction of landfalling hurricanes with the Advanced Hurricane WRF model." *Monthly weather review* 136.6 (2008): 1990-2005.

[5] Donelan, M. A., et al. "On the limiting aerodynamic roughness of the ocean in very strong winds." *Geophysical Research Letters* 31.18 (2004).

[6] Taylor, Peter K., and Margaret J. Yelland. "The dependence of sea surface roughness on the height and steepness of the waves." *Journal of physical oceanography* 31.2 (2001): 572-590.

Appendix E: Project Newsletter Jan - July 2014

January 2014

1) Interview for the last two candidates occurred at Risø DTU. Four supervisors all voted for Jing Ting Du from the first Oceanography Institute of China. He already has experience in coupling the ocean and wave model MASNUM-WAM with WRF and he seems skillful in computing. We are going through the paper work to get approval from DTU PhD committee. The earliest committee meeting is on 22nd Feb 2014. Meanwhile, Jian Ting Du needs to apply for a job visa. Let me know if you want to know more about the candidate.

2) Joakim has left the project and is pursuing a career in Norway. There are a few ideas to be tested regarding the offline coupling. All in all, the offline coupling experiments so far can be considered successful.

3) Alastair sent in an updated report for WRF-WAM coupling using MCEL.

4) The Interim report for the first project phase has been submitted to Energinet.dk, together with detailed budget. The report was prepared by Xiaoli, Rodolfo and Alastair.

Feb.-March 2014

1) X-WiWa project is connected to a newly funded EU project called IRPWIND, where we made a connection with Athens University – they are running SKIRON and WAM.
2) X-WiWa was referred to by a DTU proposal (lead by Alfredo), which will use lidars to measure coastal flows over the water, together with DHI's experiment. There seems to be a rather high chance to get this project funded - if so, we will have some measurements as input to X-WiWa, and we should make sure they capture at least one storm.
3) Mark spoke with John Michalakes at NCAR and learned some more about the coupling using ESMF – the information will be shared with the rest of group soon.
4) Xiaoli went to the conference of Danish Research Consortium for Wind Energy (26th March, Herning, Denmark) and had a presentation about X-WiWa and some preliminary results. A poster was presented as well. I am sure we will have more to show next year.

April - May 2014

1) From 15th April, Jianting Du becomes a PhD student at Wind Energy Department, DTU.

2) We made a study plan for Jianting, as required by DTU. At this moment he is learning MIKE 21 SW and experimenting with offline coupling (single domain + nested domain in WRF). He will attend the WRF tutorial in July.

3) Mark visited NCAR in May and spoke with EMSF experts and made connections, which will help Jianting's visit.

4) In May 15 – 16, Søren Larsen and Xiaoli went to the mini-workshop "air-sea interaction" at Uppsala University where people showed latest findings of swell (Uppsala University) and storms (Miami University) through measurements. We talked about possible collaboration with Uppsala University, Miami University and Helsinki University.

5) Rodolfo and Xiaoli are analyzing the modeled data (offline coupling) and measurements from Horns Rev, preparing for the International conference on coastal engineering, 2014.

6) Due to the delay of Jianting's position, we are a bit delayed in obtaining results. This leads to the fact that we will have our next meeting beginning of September.

June – July 2014

1. DTU and DHI had small project meetings related to (1) detailed technical issues regarding coupling WRF and MIKE. (2) PhD project plan

2. DTU submitted the PhD study plan to be evaluated.

3. DHI has been facilitating the PhD student Jianting to MIKE software with previous implementations.

4. Jianting attended WRF tutorial in Boulder in July.

5. Jianting completed the nested coupling using WRF and MIKE and the improvement is obvious compared to single-domain case. He prepared a report for this and it is included in the Interim report for Energinet.dk.

6. Rodolfo attended the International conference on coastal engineering (ICCE, http://icce2014.com/home/) for which he summarized some of X-WiWa's output in a conference paper.

7. MIKE source code has been made available to one of DHI X-WiWa partners.